Long-time Solutions of the Ostrovsky Equation

By Roger Grimshaw and Karl Helfrich

The Ostrovsky equation is a modification of the Korteweg-de Vries equation which takes account of the effects of background rotation. It is well known that the usual Korteweg-de Vries solitary wave decays and is replaced by radiating inertia gravity waves. Here we show through numerical simulations that after a long-time a localized wave packet emerges as a persistent and dominant feature. The wavenumber of the carrier wave is associated with that critical wavenumber where the underlying group velocity is a minimum (in absolute value). Based on this feature, we construct a weakly nonlinear theory leading to a higher-order nonlinear Schrödinger equations in an attempt to describe the numerically found wave packets.

1. Introduction

Commonly occuring internal solitary waves in the oceans have been described with remarkable success by Korteweg-de Vries (KdV) theory and its various extensions (see [2] and references therein). Some of the most important of these extensions include the roles of variable topography and stratification, friction, higher-order nonlinearity, and rotation. The last of these, in particular, introduces some interesting effects and is the subject of this paper. The KdV equation was first extended to include weak rotation by Ostrovsky [6] and the resulting equation (see equation (1) below) has become known as the Ostrovsky

Address for correspondence: Roger Grimshaw, Centre for Nonlinear Mathematics and Applications, Department of Mathematical Sciences, Loughborough University, UK; e-mail: R.H.J.Grimshaw@lboro.ac.uk

STUDIES IN APPLIED MATHEMATICS 121:71–88

Published by Blackwell Publishing, 350 Main Street, Malden, MA 02148, USA, and 9600 Garsington Road, Oxford, OX4 2DQ, UK.

equation. The most significant aspect of the rotation in the oceanographic problem is that it eliminates the steady solitary waves solutions [5]. KdV solitary waves inserted as an initial conditions in the Ostrovsky equation decay in finite time through a resonance between the solitary waves and the inertia-gravity waves introduced into the system by rotation [1]. As the solitary wave propagates it slowly looses energy into the longer rotational waves which trail the primary solitary wave. Further, an interesting recurrence phenomenon was observed. Although the initial solitary wave decayed by radiation, a radiated inertia-gravity wave, of sufficiently large amplitude, could itself steepen and produce a secondary solitary wave, which in turn decayed. This cycle was then repeated.

In a recent numerical study of a fully-nonlinear, weakly dispersive model of internal solitary waves in a rotating two-layer system this near-recurrence phenomenon was investigated numerically in more detail. It was was found that when these solutions were continued for a long enough time, this decay and re-emergence cycle eventually produced a new persistent feature [3]. Again, the initial solitary wave decayed through the radiation of intertia gravity waves. Then the radiated long waves undergo a nonlinear steepening process from which a new solitary-like wave emerges at the expense of the first wave. This decay and re-emergence process then repeats. Eventually, a nearly localized wave packet emerges, consisting of a longwave envelope through which shorter, faster solitary-like waves propagate. The dynamics of this long-time behavior was not explained in [3]. The resemblence of packets to packet solitons of the nonlinear Schrodinger (NLS) equations is suggestive of the underlying dynamics and motivates this paper. However, rather than work with the more complicated fully-nonlinear governing equations employed in [3], we will explore the long-time behavior of the Ostrovsky equation. It can be found in the weakly-nonlinear limit of the full set, and is much simpler to analyze.

The Ostrovsky equation is

$$\{\eta_t + \nu\eta\eta_x + \lambda\eta_{xxx}\}_x = \gamma\eta. \tag{1}$$

Our concern here is for the case when $\lambda\gamma > 0$ when it is known that (1) does not support steady solitary wave solutions (see [5], or [1] and the references therein). Without loss of generality, we may choose $\nu > 0$, $\lambda > 0$, $\gamma > 0$. Our numerical results, described below in Section 3, suggest that the localized wave packet that eventually emerges has the slowest speed of all the emitted radiation, that is, in a weakly nonlinear analysis, it propagates with the smallest (in absolute value) group velocity.

Equation (1) has the linear dispersion relation,

$$c = \frac{\gamma}{k^2} - \lambda k^2, \tag{2}$$

for sinusoidal waves of wavenumber k, frequency ω and phase velocity $c = \omega/k$. The corresponding group velocity is

$$c_g = \frac{d\omega}{dk} = -\frac{\gamma}{k^2} - 3\lambda k^2. \tag{3}$$

This is negative for all wavenumbers k, and has a local maximum where $dc_g/dk = 0$ at $k = k_c$ where $3\lambda k_c^4 = \gamma$; the local maximum is $c_g = -2\gamma/k_c^2 = -2\sqrt{3\gamma\lambda}$. Note that as γ increases so does k_c, $|c_g|$. Hence, in developing a theory to describe the wave packet, we focus our attention on this critical wavenumber k_c. In the next Section 2, we present a theory for these wave packets, which need a higher-order version of the usual NLS equation. Then in Section 3, we present our numerical results. In Section 4, we conclude with a discussion of the comparison between the theory and the numerical results.

2. Higher-order nonlinear Schrödinger equations

2.1. Envelope solitary wave

In a wide variety of physical systems, the usual NLS equation is

$$i(A_t + c_g A_x) + \Delta A_{xx} + \mu|A|^2 A = 0. \tag{4}$$

for the complex envelope $A(x.t)$ of the weakly nonlinear solution

$$\eta = A(x, t)\exp(ikx - i\omega t) + \text{c.c.} + \cdots, \tag{5}$$

where c.c. denotes the complex conjugate. Here $\omega = \omega(k)$ satisfies the linear dispersion relation and at leading order the envelope moves with the linear group velocity $c_g = \omega_k$. The dispersive term in (4) generically has the coefficient $\Delta = c_{gk}/2$, but the coefficient μ of the cubic nonlinear term is system-dependent.

Our concern here is with the situation when $\Delta = c_{gk}/2 = 0$, selecting a wavenumber $k = k_c$ where the group velocity has a local extremum. In this case we must replace the NLS equation (4) with

$$i(A_t + c_g A_x) + \Delta A_{xx} + i\delta A_{xxx} + \mu|A|^2 A = 0, \tag{6}$$

where $\delta = -c_{gkk}/6 \neq 0$ is the coefficient of the third-order linear dispersive term. Note that we retain Δ, even although it may be zero, to broaden the parameter space. Equations of this type have arisen in nonlinear optics where it has been found advantageous to include as well the next order nonlinear terms (see, for instance, [4, 7]). Thus we extend (6) to

$$i(A_t + c_g A_x) + \Delta A_{xx} + i\delta A_{xxx} + \mu|A|^2 A + i\left(\alpha|A|^2 A_x + \beta A^2 A_x^*\right) = 0. \tag{7}$$

Here * denotes the complex conjugate. Technically the terms with coefficients α, β are higher order, but nevertheless they are needed, as follows.

We seek a solitary wave solution of the form,

$$A = F(X - Vt)\exp(i\kappa X - i\sigma t), \quad X = x - c_g t, \tag{8}$$

where we choose the gauge κ and the chirp σ so that

$$\mu + 2\kappa\beta = \frac{(\alpha+\beta)\Delta}{3\delta}, \quad \sigma = 3\kappa V + 8\delta\kappa^3 + \frac{\Delta}{\delta}(4\delta\kappa^2 - V) - \frac{2\kappa\Delta^2}{\delta}. \tag{9}$$

Note that when $\Delta = 0$, $\kappa = -2\mu/\beta$. Then $F(X)$ is real-valued and satisfies the equation

$$\delta F_{XX} - \tilde{V}F + \frac{\alpha+\beta}{3}F^3 = 0, \quad \tilde{V} = V + 3\delta\kappa^2 - \Delta\kappa. \tag{10}$$

This has a "sech"-solitary wave solution, provided that $\tilde{V} > 0$ (a suitable choice of V can always achieve this condition), and $\delta(\alpha + \beta) > 0$. Note that the higher-order nonlinear terms are needed to get this solution. Explicitly

$$F = a\,\mathrm{sech}(KX), \tag{11}$$

$$\text{where} \quad \tilde{V} = \delta K^2 = \frac{a^2(\alpha+\beta)}{6}. \tag{12}$$

The next step is to derive the envelope equation (7) from the Ostrovsky equation (1), and hence obtain the envelope solitary wave solution (11) in terms of the coefficients of (1). This derivation is described in Section 2.2. Here we recall from Section 1 (see (2, 3)) that for the Ostrovsky equation (1) there is a unique $k = k_c$, $3\lambda k_c^4 = \gamma$, where $c_{gk} = 0$ and where $c_g = -2\gamma/k_c^2 = -2\sqrt{3\gamma\lambda}$ is a maximum. Hence we can indeed derive an extended NLS equation (7) for this wavenumber, with the main aim of finding the sign of $\alpha + \beta$. Note that for (1) $\Delta = \gamma/k^3 - 3\lambda k$, and so $\Delta > 0$ (<0) according as $k < k_c (k > k_c)$; also $\delta = \gamma/k^4 + \lambda > 0$ for all k, and at criticality $\delta = 4\lambda$.

2.2. Derivation of the envelope equation

For the Ostrovsky equation (1) we seek an asymptotic expansion, compare (5),

$$\eta = A\exp i\theta + \text{c. c.} + A_2\exp 2i\theta + \text{c. c.} + A_0 + \cdots, \tag{13}$$

$$\text{where} \quad \theta = kx - \omega t, \tag{14}$$

Here it is understood that $A(x, t)$, etc. are slowly varying, while we expect that the second harmonic A_2 and the mean term A_0 are $O(|A|^2)$ where $|A| \ll 1$.

The leading order term yields the dispersion relation in the form

$$D(\omega, k) = \omega k + \lambda k^4 - \gamma = 0. \tag{15}$$

Then the leading order terms in the coefficient of the first harmonic yield

$$D\left(\omega + i\frac{\partial}{\partial t}, k - i\frac{\partial}{\partial x}\right) A + \left(k - i\frac{\partial}{\partial x}\right) \mathrm{NL} = 0, \tag{16}$$

where the nonlinear term NL is given by

$$\mathrm{NL} = -\nu \left(k - i\frac{\partial}{\partial x}\right) \left(A_2 A^* + A_0 A + \cdots\right). \tag{17}$$

Expanding and noting that $D_\omega = k$ gives

$$i(A_t + c_g A_x) + \Delta A_{xx} + i\delta A_{xxx} + \mathrm{NL} + \cdots = 0, \tag{18}$$

where $\Delta = c_{gk}/2$, $\delta = -c_{gkk}/6$ as before. It remains to find the nonlinear term NL.

First we note that to leading order

$$\gamma A_0 - A_{0xt} + \cdots = \nu |A|^2_{xx} + \cdots. \tag{19}$$

Hence A_0 is two orders of magnitude smaller than $|A|^2$, provided that $\gamma \neq 0$. Hence it can be neglected henceforth. However note that if $\gamma = 0$ then $A_0 = \nu|A|^2/c_g$ and is then of the same order as $|A|^2$. Also, if $\gamma \ll 1$, then the solution for A_0 is again of the same order as $|A|^2$, but is nonlocal. Henceforth we assume that $\gamma \neq 0$ and is $O(1)$, because then k_c is also $O(1)$.

Next

$$D\left(2\omega + i\frac{\partial}{\partial t}, 2k - i\frac{\partial}{\partial x}\right) A_2 = \frac{\nu}{2}\left(2k - i\frac{\partial}{\partial x}\right)^2 A^2. \tag{20}$$

To the leading order

$$D_2 A_2 = 2\nu k^2 A^2, \tag{21}$$

$$\text{where} \quad D_2 = D(2\omega, 2k) = 12\lambda k^4 + 3\gamma (= 7\gamma). \tag{22}$$

Here the term in brackets is the value at criticality. However because we need the next order terms as well,

$$D_2 A_2 = 2\nu k^2 A^2 - 2i\nu k (A^2)_x - i D_\omega(2\omega, 2k) A_{2t} + i D_k(2\omega, 2k) A_{2x} + \cdots, \tag{23}$$

where in the last two terms on the right-hand side we may now substitute the leading-order expression for A_2. The outcome is

$$D_2 A_2 = 2\nu k^2 A^2 + i C_2 (A^2)_x + \cdots, \tag{24}$$

$$\text{where} \quad C_2 = -2\nu k + 4\nu k^3 \frac{[c_g(k) - c_g(2k)]}{D_2} = \frac{\nu k [12\lambda k^4 - 9\gamma]}{12\lambda k^4 + 3\gamma} \left(= -\frac{5\nu k_c}{7}\right). \tag{25}$$

Hence, on substituting (24) into (17) we find that

$$\text{NL} = -\nu k A_2 A^* + i\nu (A_2 A^*)_x + \cdots, \tag{26}$$

$$\text{and thus} \quad \text{NL} = \mu |A|^2 A + i\alpha |A|^2 A_x + i\beta A^2 A_x^*, \tag{27}$$

$$\text{where} \quad \mu = -\frac{2\nu^2 k^3}{D_2}, \tag{28}$$

Note that $\mu < 0$ for all k and thus the NLS here is focussing for $k > k_c$ and defocussing for $k < k_c$ where k_c is where $c_{gk} = 0$; this is in sharp contrast to the usual KdV case ($\gamma = 0$) when the NLS is always defocussing. The reason is twofold, first that the presence of rotation has suppressed the mean flow, and hence changed the sign of μ from the KdV case, and secondly it has introduced the critical turning point $k = k_c$.

The higher-order coefficients are given by

$$\alpha = -\frac{2\nu k C_2}{D_2} + \frac{4\nu^2 k^2}{D_2} = \frac{2\nu^2 k^2 (12\lambda k^4 + 15\gamma)}{(12\lambda k^4 + 3\gamma)^2} \left(= \frac{38\nu^2 k_c^2}{49\gamma} \right). \tag{29}$$

$$\beta = \frac{2\nu^2 k^2}{D_2} \left(= \frac{2\nu^2 k_c^2}{7\gamma} \right). \tag{30}$$

Thus both $\alpha, \beta > 0$ for all k, confirming that an envelope soliton of the kind described in Section 2 by (11) exists for $k = k_c$. Further, because $\mu < 0$, it follows that $\kappa = k_c/2 > 0$ at criticality, and thus then the actual wavenumber for the carrier wave is $k_c + \kappa = 3k_c/2 > k_c$. However, above criticality ($k > k_c$, $\Delta < 0$) it follows from (9) that κ decreases as k increases above k_c. Indeed, we note here that for the wavenumber $k_0 = (\gamma\lambda)^{1/4}$ where the phase speed $c = 0$, $\alpha/\beta = 9/5$, $\Delta = -2\lambda k_0$, $\delta = 2$ and thus from (9) we find that $\kappa = k_0/30$.

Before proceeding with our main numerical results in Section 3, we note that we can use the the wave packet solution, given by (8, 11), as an initial condition. The result, for the case of criticality, $k = k_c$, is shown in Figure 1. Clearly the solution persists, and confirms the asymptotic validity of the constructed wave packet.

3. Numerical results

First note that the transformation

$$x = L\tilde{x}, \quad t = T\tilde{t}, \quad \eta = M\tilde{\eta}, \quad \text{with} \quad L^4 = \frac{\lambda}{\gamma}, \quad T = \frac{L^3}{\lambda}, \quad M = \frac{\lambda}{\nu L^2}, \tag{31}$$

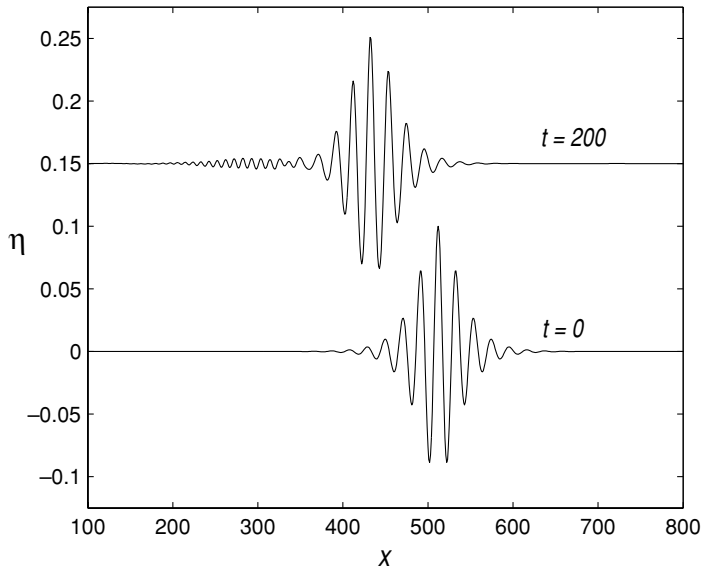

Figure 1. Numerical solution of the Ostrovsky equation for the initial condition of a wave packet given by (8, 11), at criticality $k = k_c$. Here $\lambda = \nu = 1$, $\gamma = 0.01$ and the wave packet initial amplitude is $a = 0.1$.

takes the Ostrovsky equation into itself, but with all coefficients equal to unity. That is, we can replace (1), after omitting the "tilde" symbol, by

$$\{\eta_t + \eta\eta_x + \eta_{xxx}\}_x = \eta. \tag{32}$$

Thus the envelope solitary wave asymptotic solution contains only one parameter, namely $\tilde{\epsilon}$ which measures the amplitude, and the ratio of the carrier wavelength to that of the envelope, see (12). Note that in these transformed coordinates the critical wavenumber is now $k_c = (1/3)^{1/4} = 0.760$, and thus the length scale of the carrier wave is $2\pi/k_c = 8.27$. Similarly, we find that in the transformed system, at criticality denoted by the subscript "c,"

$$\delta_c = 4, \quad \mu_c = -0.125, \quad \alpha_c = 0.448, \quad \beta_c = 0.165. \tag{33}$$

All that is now required in the transformed equation (32) for the validity of the envelope solitary wave asymptotic solution is that the transformed amplitude be sufficiently small. Note that from (12) the wavenumber parameter $K = 0.0255a$ where a is now the transformed wave amplitude. Thus the ratio of the carrier wavelength to the envelope width is $2\pi K/k_c = 0.211\,a$, and this is also a measure of the small expansion parameter.

Thus we can use the wave amplitude, denoted now by $\tilde{\epsilon} \ll 1$, as the expansion parameter. In the original variables, the (implicit) amplitude

expansion parameter is $\epsilon = M\tilde{\epsilon}$ and thus the condition for the validity of the envelope solitary wave asymptotic solution is

$$\epsilon \ll M, \quad \text{or} \quad \epsilon \ll \frac{\sqrt{\lambda\gamma}}{\nu}. \tag{34}$$

Thus, as our numerical solutions (but not shown here) indicate, the amplitude scales with $\sqrt{\gamma}$. Thus in the original equation (1) the smaller γ, the more difficult it becomes to find an envelope solitary wave. However the difficulty can be avoided by using the transformed equation (32) instead.

However, we need to note that when using the KdV sech^2-profile as an initial condition, the dependence on γ re-emerges in the transformed equation and is now in the initial condition. That is

$$\eta = a_0 \mathrm{sech}^2(x/D), \quad \nu a_0 D_0^2 = 12\lambda, \tag{35}$$

$$\text{becomes} \quad \tilde{\eta} = \tilde{a_0}\mathrm{sech}^2(\tilde{x}/\tilde{D_0}), \quad \text{where} \quad a_0 = M\tilde{a_0},$$

$$D_0 = L\tilde{D_0}, \quad \tilde{a_0}\tilde{D_0}^2 = 12. \tag{36}$$

Thus for a given input amplitude a_0, $\tilde{a_0}$ varies as $\gamma^{-1/2}$ and $\tilde{D_0}$ as $\gamma^{1/4}$. As γ decreases, the input becomes larger and narrower.

Numerical solutions of the transformed Ostrovsky equation (32) were obtained using a psuedo-spectral method in x and an Adams-Bashforth-Moulton predictor-corrector integration in t. The solutions are thus periodic in x. To prevent the possibility of radiated waves from re-entering the domain the scheme adds a linear damp (sponge) region at each end of the domain. The runs are initiated with the KdV solitary wave with amplitude a_0 between 1 and 32 (the "tilde" is omitted here and henceforth).

Numerical runs with $a_0 = 2$, 4, 8, 16, and 32 are shown in Figures 2–6. In all these cases a leading wave packet forms. However, for $a_0 = 2$ and 4, the packet does not completely separate from the trailing radiation at the end of the calculation. For the larger initial amplitudes (Figures 4–6) the separation of a leading packet is clear. In all these cases the leading disturbance amplitude has reached a steady, or nearly steady, state. Figure 7 shows the maximum and minimum amplitude of the solution with time. Note that when following one of the sequence of amplitudes for a given run only the largest (smallest) values are important as they indicate the amplitudes of the envelope.

A close-up plot of the leading packets in each of these examples is shown in Figure 8. All the solutions have the character of the extended NLS envelope solutions. However, as the amplitude of the initial wave, and the resulting packet increases, the packets become increasingly asymmetric with the maximum amplitude greater than the magnitude of the minimum amplitude as shown in Figure 7. For $a_0 = 16$, 32 the leading packets are qualitatively such as those found in [3]. This is perhaps to be expected because the large amplitudes

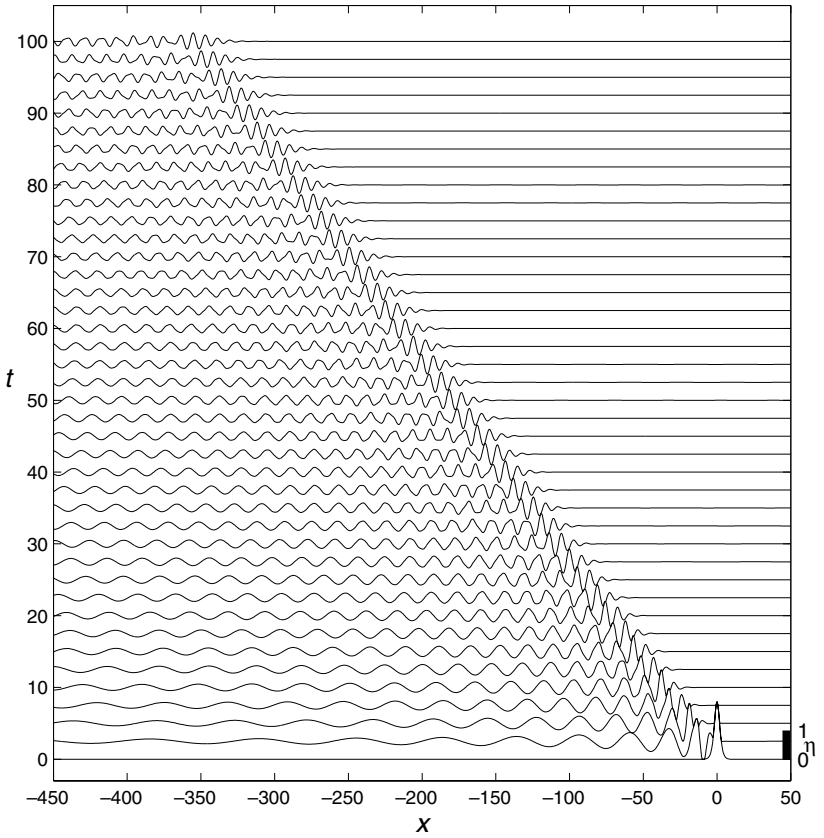

Figure 2. Numerical solution of the Ostrovsky equation for an initial condition given by a KdV solitary wave with $a_0 = 2$ at $x = 0$. Note that only the portion of the domain containing the leading packet is shown. The amplitude is indicated by the scale on the lower right.

are equivalent to small γ for fixed a in the original Ostrovsky scaling and the numerical solutions in [3] were in the small γ (weak rotation) regime. The wavenumbers of the carrier waves in the leading packets are all close to $k_c + \kappa$, though the trend is for the wavenumber to increase with increasing amplitude, whereas the theory predicts that it should stay constant.

A quantitative comparison of the packet propagation speed V (relative to the group speed $c_{gc} = c_g(k_c)$ at criticality $k = k_c$) from the numerical solutions and the theory is given in Figure 9. The theoretical prediction for V is from (10) and (12) with the rescaled coefficients (33). The packet speeds are approximately equal to $c_{gc}(V \approx 0)$ with only a very weak dependence on amplitude; this in sharp contrast to the theoretical prediction that the speed increases as the square of the amplitude. A similar disagreement is found for the packet wavenumber, which from the theory is $K = 0.0255a$. The packets

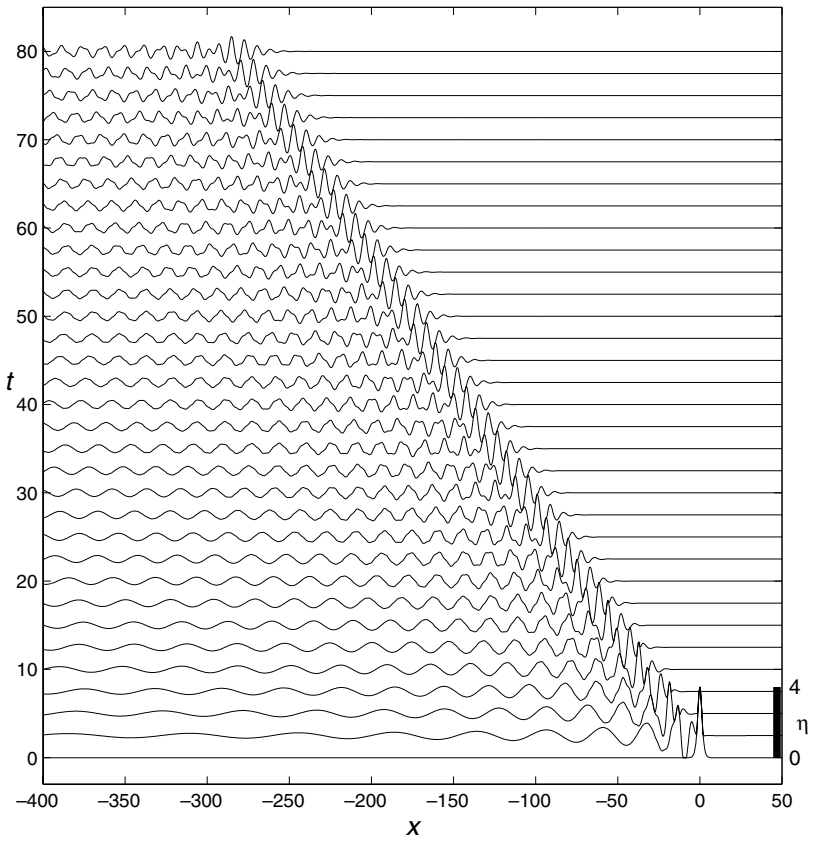

Figure 3. The same as Figure 2, except $a_0 = 4$.

shown in Figure 8 all have approximately the same width scale over an $O(10)$ variation in a. Thus while the presence of leading wave packets with carrier waves near k_c is qualitatively what one might expect from the theory, the quantitative agreement is not very good. Possible reasons for this are discussed in the next section

4. Discussion

4.1. Decaying solitary wave

We need now to discuss how the initial KdV solitary wave transforms to an envelope solitary wave, why the carrier wavenumber is selected to be k_c and what determines the packet amplitude a. To do this at first we follow the asymptotic argument of [1], where γ is a small parameter, but expect that at least qualitatively the outcome may hold when γ is finite, but not too large.

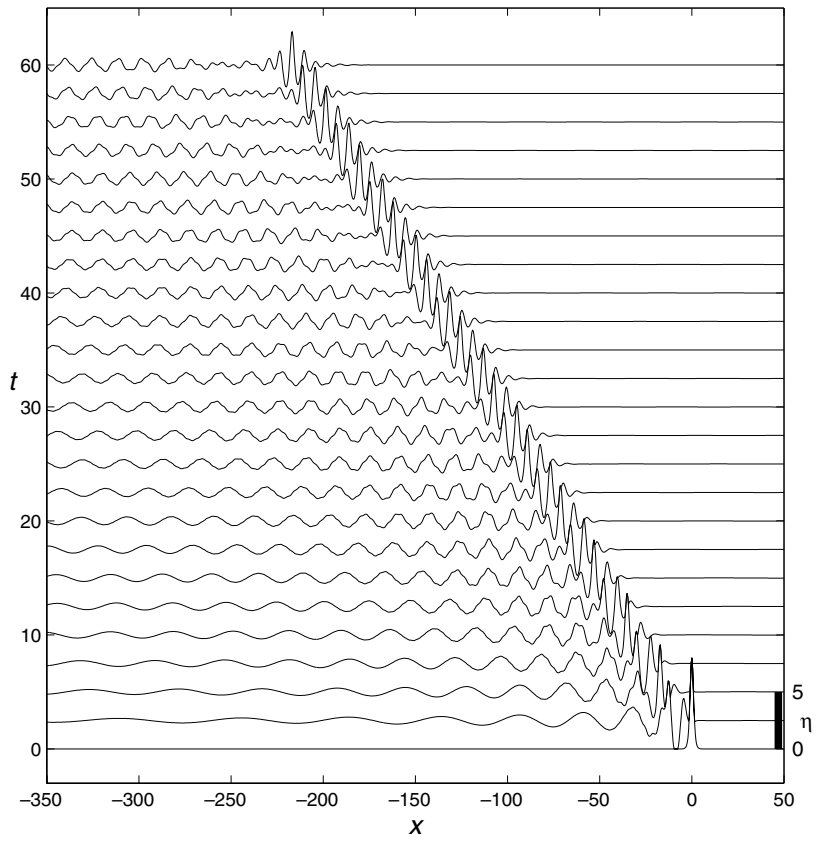

Figure 4. The same as Figure 2, except $a_0 = 8$.

Thus we assume the following asymptotic form for the decaying solitary wave solution of (1),

$$\eta \sim \eta_s = a_s \operatorname{sech}^2\left(\frac{x - P(t)}{D}\right), \quad V_s = P_t = \frac{\nu a_s}{3} = \frac{4\lambda}{D^2}. \tag{37}$$

The determination of how $a(t)$ decays is found from the "energy" law

$$\frac{d}{dt}\int_{-\infty}^{\infty} \eta^2\, dx = -\gamma\left(\int_{-\infty}^{\infty} \eta\, dx\right)^2, \tag{38}$$

For the full Ostrovsky equation (1) the right-hand side is zero, as the equation carries zero "mass." However here we apply this locally to the solitary wave (37), with the balance of the total energy being carried away in radiated waves. Hence we find that

$$\frac{d\left(a_s^2 D\right)}{dt} = -6\gamma a_s^2 D^2 \quad \text{or} \quad \frac{da_s}{dt} = -4\gamma\sqrt{\frac{12\lambda a_s}{\nu}}. \tag{39}$$

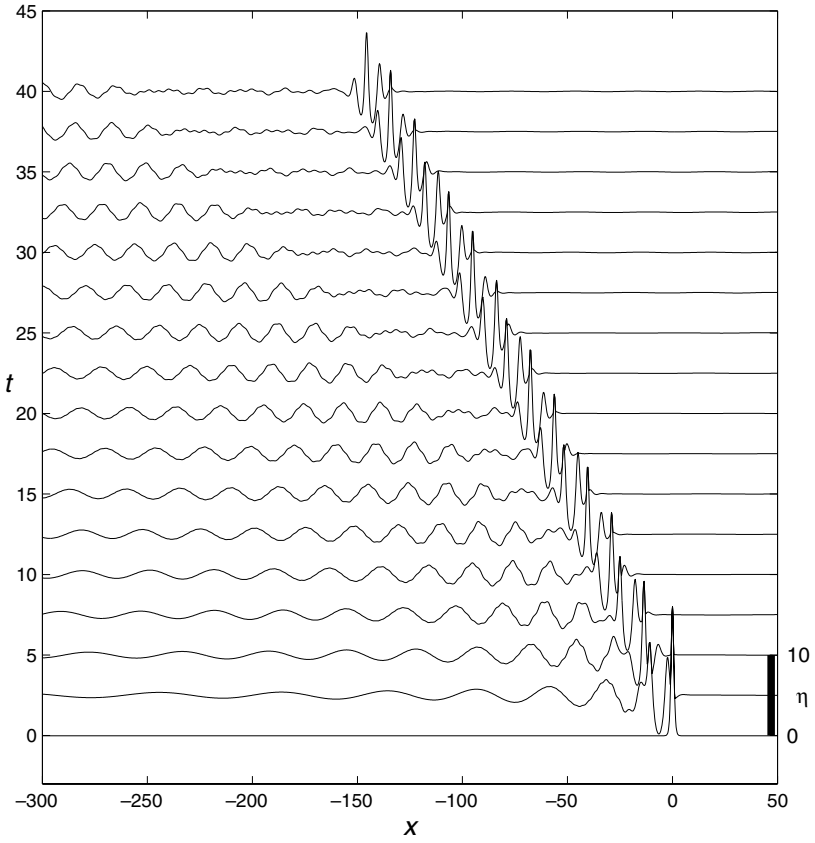

Figure 5. The same as Figure 2, except $a_0 = 16$.

This has the solution

$$a_s^{1/2} = a_0^{1/2} - \Gamma t, \quad \Gamma = 2\gamma\sqrt{\frac{12\lambda}{\nu}}. \tag{40}$$

Thus the solitary wave is extinguished in finite time t_0, proportional to $a_0^{1/2}/\gamma$, where a_0 is the initial amplitude. In the transformed variables, leading to (32), the extinction time is $t_0 = \sqrt{12a_0}/2$. Note that in our numerical simulations, for the range of initial amplitudes a_0 that we consider, this time is very short compared to the total run time. Using the expression (37) and (40) we find that

$$P(t) = \frac{\nu a_0^{3/2}}{9\Gamma} - \frac{\nu}{9\Gamma}\left(a_0^{1/2} - \Gamma t\right)^3. \tag{41}$$

The location of the extinction point is $x = P_0 = P(t_0) = \nu a_0^{3/2}/9\Gamma$.

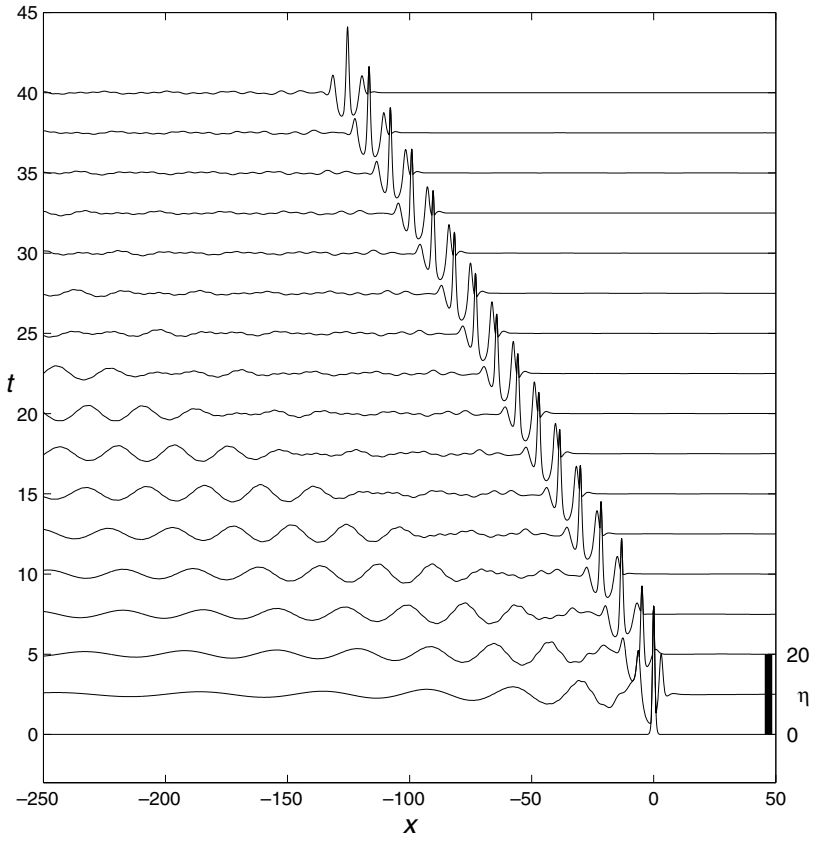

Figure 6. The same as Figure 2, except $a_0 = 32$.

4.2. Radiated waves

As the solitary wave decays, it propagates along the path $x = P(t)$, emitting radiation to the left, because the group velocity for linear waves is negative for all wavenumbers. Although in the very long-time limit weakly nonlinear effects will emerge, we analyze this radiated wave field using the linearized Ostrovsky equation, with the aim of establishing what wavenumbers may be preferred and what wave amplitudes may be associated with that wavenumber. The linear dispersion relation is given by (2) so that the phase speed c and the group velocity c_g are given by (2) and (3) respectively. At the solitary wave location $x = P(t)$, the emitted wave will then have that wavenumber $k_P(t)$ determined by $c = c_P(t) = V_s(t)$. For $0 < t < t_0$, it follows that $V_s(0) > c_P > 0$ and thus $k_P(0) < k_P < k_0 = (\gamma/\lambda)^{1/4}$. Note that for small γ only long waves are emitted. The radiation field can then be determined using linear kinematic wave

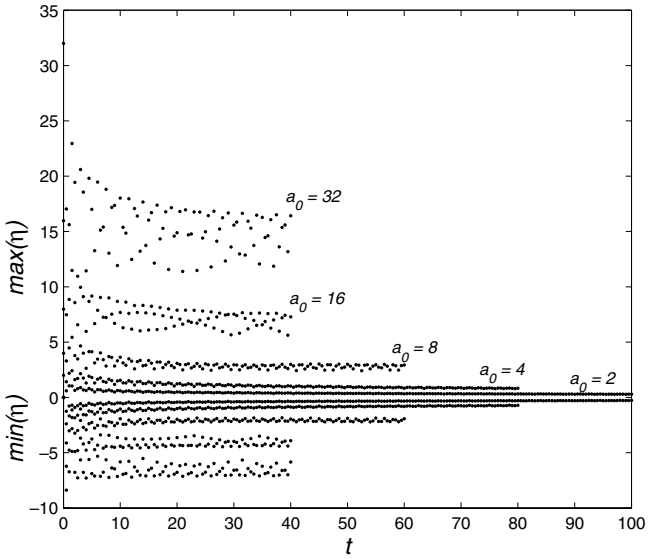

Figure 7. Maximum and minimum wave amplitude for the solutions in Figures 2–6 versus t.

theory. This was the procedure used by [1]. Here, however, we will proceed in a slightly different way, because we have the expectation that the wavenumber k_c will be selected preferentially, and in the linear kinematic wave theory, this wavenumber is exceptional in being connected to the formation of a caustic, which is not strictly contained within that theory. However before proceeding we note that to excite the wavenumber k_c, we must ensure that $V_s(0) > c_c$, the phase speed at criticality, given by $c_c = c(k_c) = 2\sqrt{\lambda\gamma/3}$. It follows that in the transformed system (32), our initial KdV solitary wave must have an amplitude $a_0 > 3.46$. Our numerical results for $a_s(0) = 2$ fail this criterion, and those for $a_s(0) = 4$ only just exceed it, thus explaining why there is little separation of the leading wave packet from the trailing radiation in these cases.

Thus we expect the radiation field to be initially described by the linearized Ostrovsky equation, with a boundary condition on $x = P(t)$ determined by matching with the decaying solitary wave. This is done as in [1] using the conservation of mass in the Ostrovsky equation. The outcome is

$$V_s \eta_x(x = P(t), t) = \gamma \int_{-\infty}^{\infty} \eta_s \, dx = 2\gamma \sqrt{\frac{12\lambda a_s}{\nu}}. \tag{42}$$

$$\eta_x(x = P(t), t) = \frac{6\gamma}{\nu} \sqrt{\frac{12\lambda}{\nu a_s}}, \tag{43}$$

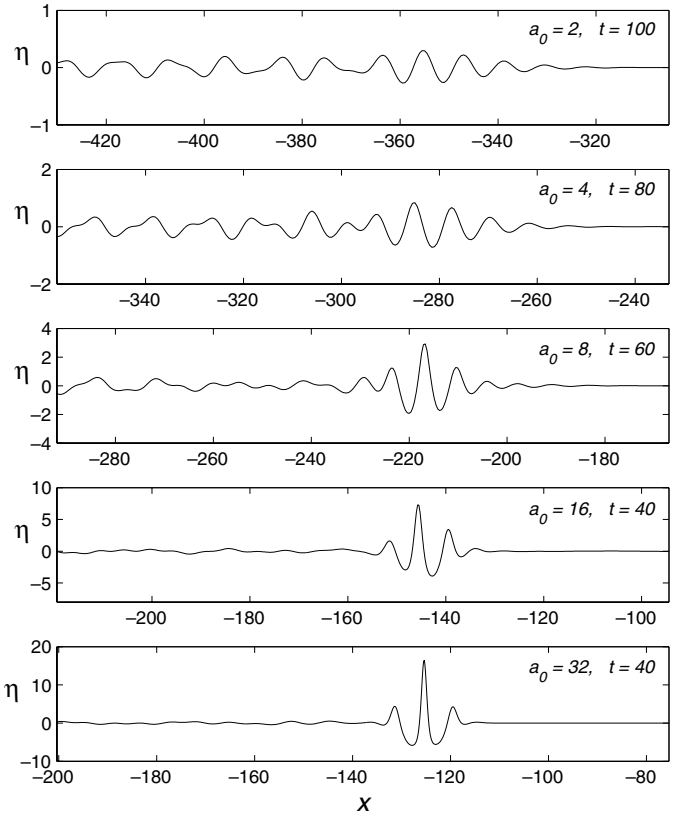

Figure 8. Leading packets at the end of the solutions in Figures 2–6.

where we recall that the solitary wave amplitude a_s is given by (40). For the radiated field, the initial condition is zero, and thus we must solve this initial-boundary-value problem for the linearized Ostrovsky equation in the domain $x < P(t)$, $t > 0$. Although this is possible in principle, because we are concerned only with the long-time outcome, it is simpler to convert the problem approximately to an initial value problem for the variable $\zeta = \eta_x$ by projecting the boundary data on $x = P(t)$ onto the axis $t = 0$. Thus we replace (43) with

$$\zeta(x, t = 0) = \frac{6\gamma}{\nu}\sqrt{\frac{12\lambda}{\nu a_s}} \quad \text{for} \quad 0 < x < P_0, \tag{44}$$

and is zero elsewhere. Using the expression (40) we find that over the interval $0 < x < P_0$, $\zeta(x, t = 0)$ is proportional to $(P_0 - x)^{-1/3}$.

This initial value problem for ζ is readily solved in a standard manner using Fourier transforms, and the outcome is

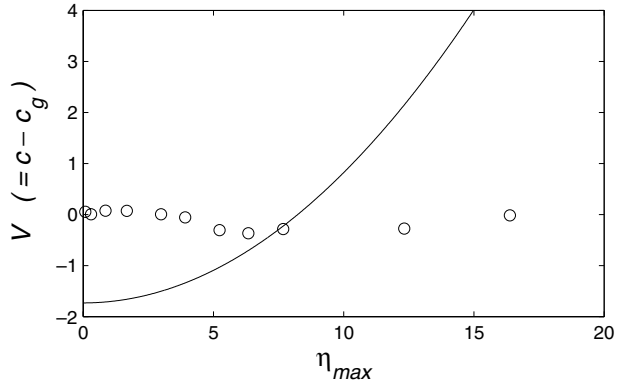

Figure 9. Packet propagation speed V from the theory (line) and numerical runs (circles) versus the packet amplitude $\eta_{\max}$ (=2a).

$$\zeta = \frac{1}{2\pi}\int_{-\infty}^{\infty} Z(k)\exp\left(ikx - ikc(k)t\right)dk, \tag{45}$$

$$Z(k) = \int_{-\infty}^{\infty} \zeta(x, t=0)\exp\left(-ikx\right)dx, \tag{46}$$

where $c(k)$ satisfies the linear dispersion relation (2), and $Z(k)$ is known from (44). The long-time limit is now found using the method of stationary phase which shows that the solution disperses as $t^{-1/2}$, except for those wavenumbers around the critical wavenumber $k = k_c$, where the dispersion is only $t^{-1/3}$. The amplitude of this dominant component is proportional to $Z(k_c)$ and our concern is how this depends on the initial amplitude a_0 We find that

$$Z(k_c) \propto \int_0^{k_c P_0} \frac{\exp\left(ix\right)}{x^{1/3}}\,dx \propto \int_0^{(k_c P_0)^{2/3}} \exp\left(iy^{3/2}\right)dy, \tag{47}$$

where only the dependence on a_0 is retained; note that $P_0 \propto a_0^{3/2}$ (in the transformed equation (32), $k_c P_0 = k_c a_0^{3/2}/36\sqrt{3}$). In general, as $a_0 \to 0$, $|Z(k_c| \propto a_0$, but then reaches a maximum value when $a_0 \approx 36$, after which it oscillates with a period of approximately π and a slowly decreasing amplitude reaching a constant value as $a_0 \to \infty$. However, in our range of interest, $Z(k_c)$ is essentially a monotonically increasing function of a_0, with only a slight departure from a linear dependence when $a_0 = 32$. This predicted trend is consistent with our numerical results, see Figure 7.

4.3. Conclusion

In summary, the theory described above predicts a carrier wavenumber $k = k_c$, with a consequent envelope speed approximately given by $c_{gc} = c_g(k_c)$, and an envelope amplitude a which increases monotonically and almost linearly with the initial solitary wave amplitude a_0 over the range $0 < a_0 < 32$. This is in broad agreement with the numerical results. However, the envelope solitary wave solution described in Section 2.1 requires that there is a correction V (12) to the linear speed c_{gc}, which increases with the square of the envelope wave amplitude. This feature is not seen at all in the numerical results, see Figure 9. However, we note that while $c_g = -2\sqrt{3} = -3.464$, the predicted values for $V > 4$ for $a_0 = 16, 32$, whereas strictly the theory for the envelope solitary wave requires that $V \ll |c_{gc}|$. From this perspective, only the case $a_0 = 8$, where the numerical results agree exactly with the predicted theoretical value for V, can be described well by the theory of Section 2. Essentially the cases $a_0 = 16, 32$ are too nonlinear, and, as noted above, the cases $a_0 = 2, 4$ are too small. Similar conclusions can be drawn from considerations of the numerically determined wave packet width *vis-a-vis* the theoretical prediction of K^{-1}(11, 12). Here the theory of Section 2.1 predicts that $K = 0.0255a$, whereas the numerical results show no such trend. However again, we note that the validity of the theory strictly requires that $K \ll k_c$, whereas this not the case when $a_0 = 16, 32$.

In conclusion, we believe that the numerical results shown in Figures 2–6 provide convincing numerical evidence that the outcome form a decaying KdV solitary wave is an envelope wave packet, with a wavenumber close to the critical wavenumber k_c and propagating with the associated minimum (in absolute value) group velocity. However, the weakly nonlinear envelope solitary wave theory that we have described in Section 2 is appropriate in only a limited parameter range. Essentially the initial KdV solitary wave amplitude must be large enough for a "small γ theory" to be relevant, but also small enough that a weakly nonlinear theory can be used.

References

1. R. H. J. Grimshaw, J.-M. He, and L. A. Ostrovsky, Terminal damping of a solitary wave due to radiation in rotational systems, *Stud. Appl. Math.* 101:197–210 (1998).
2. K. R. Helfrich and W. K. Melville, Long nonlinear internal waves, *Ann. Rev. Fluid Mech.* 38:395–425 (2006).
3. K. R. Helfrich, Decay and return of internal solitary waves with rotation, *Phys. Fluids* 19:026601 (2007).
4. Y. Kodama and A. Hasegawa, Nonlinear pulse propagation in a monomode dielectric guide, *IEEE J. Quantum Electronics* 23:510–524 (1987).

5. A. I. Leonov, The effect of the earth's rotation on the propagation of weak nonlinear surface and internal long oceanic waves, *Ann. NY Acad. Sci.* 373:150–159 (1981).
6. L. Ostrovsky, Nonlinear internal waves in a rotating ocean, *Oceanogology* 18(2):119–125 (1978).
7. N. Sasa and J. Satsuma, New-type of soliton solutions for a higher-order nonlinear Schrödinger equation, *J. Phys. Soc. Japan* 60:409–417 (1991).

Loughborough University
Woods Hole Oceanographic Institution

(Received March 3, 2008)